EVALUATION OF THE HYDROCARBON POTENTIAL, MINERAL MATRIX EFFECT AND GAS-OIL RATIO POTENTIAL OF OIL SHALE FROM THE KABALAR FORMATION, GÖYNÜK, TURKEY

ALI SARI[a], ARASH VOSOUGHİ MORADİ[b]*,
YAĞMUR KULAKSIZ[b], AYŞE KÜBRA YURTOĞLU[b]

[a] Department of Geological Engineering, Ankara University, Tandoğan 06100, Ankara, Turkey
[b] Graduate School of Natural and Applied Sciences, Ankara University, Keçiören 06110, Ankara, Turkey

Abstract. *The present study focuses on the evaluation of the hydrocarbon potential, retention effect of mineral matrix and the gas-oil ratio potential (GORP) of oil shale from the Kabalar Formation in the Göynük area, Turkey, to assess the quality of its organic matter. The results of Rock-Eval pyrolysis generally suggest relatively high organic carbon content (TOC) for Kabalar oil shale, ranging from 1 to 13.23 wt%. These values are consistent with data on source rocks that may have a good to excellent source rock potential. The kerogen in Kabalar oil shale was characterized based on Hydrogen Index (HI) value, S_2/S_3 ratio, and organic petrographic studies. The results indicate that most of the studied samples are characterized as containing oil prone (type I and II kerogen) organic matter. The low spore color index (SCI) and high S_2/S_3 ratio with a commonly low T_{max} (< 440 °C) demonstrate that most of the oil shale samples are in the immature to early mature stages of thermal maturity. After calculating the transformation ratio (TR), the oil shale samples were divided into mature (TR = 0.2) and immature (TR = 0) subdivisions in order to take the maturity effects on organic carbon content (TOC) and hydrocarbons retention into account and also select the appropriate GORP overlay. After correcting the mineral matrix effect in the immature subdivision, the mean HI value of the Kabalar Formation increased by about 268 and reached 855 mg HC/g TOC. Due to the relatively higher thermal maturity values, the mineral matrix effect is minimized in the mature subdivision. Based on GORP factor, the $TOC_{(live)}$ of Kabalar oil shale is composed only of oil prone material, which is in good agreement with the results inferred from organic petrographic and pyrolysis studies.*

Keywords: *oil shale, mineral matrix effect, Rock-Eval pyrolysis, gas-oil ratio potential, Göynük.*

---

* Corresponding author: e-mail *moradi@ankara.edu.tr*

1. Introduction

The energy consumption of Turkey was forecasted in 1984 to increase from 53 to 77 Mtoe (million tons of oil equivalent) from 1990 to 2001, corresponding to a rise of around 50%. On account of the growing population and increasing industrialization, the rapid growth of energy consumption was predicted to continue for the next 15 years. On the other hand, energy production in the country was 26 Mtoe in 2001 and this satisfied only 33% of the total demand [1]. Next to lignites which are used mainly for power generation in coal-fired thermal power plants, oil shales are the second largest fossil fuel potential of Turkey, which are widely distributed in middle and western Anatolia. Hence, investigating oil shales as an important energy source is vital. Oil shale deposits in Beypazarı, Seyitömer, Hatıldağ and Himmetoğlu areas are the major reserves of this rock in Turkey and have been comprehensively investigated [2–4]. In the majority of oil shale basins of Turkey the host rock is composed of consolidated marl and clays [5]. The upper calorific value and oil content of oil shale in the major deposits are generally low, ranging from 773.86 to 847.9 kcal/kg and 5 to 5.4%, respectively. However, in Himmetoğlu oil shale these values reach respectively 4991.8 kcal/kg and 30.9% [6, 7]. The geological setting and geochemistry of Göynük oil shale has also been the subject of numerous prior studies [2, 8–11]. The main aim of the present research is to provide a more realistic evaluation of the hydrocarbon potential of Kabalar oil shale by taking mineral matrix retention effect into account, using sedimentary basin-scale sampling and applying the gas-oil ratio potential (GORP) factor presented by Dahl et al. [12]. This paper also attempts to provide more accurate data (especially pyrolysis data) for assessing alternative energy prospects of the region and further scientific researches. Nowadays it is widely accepted that the amount and physicochemical characteristics of an oil reservoir found in a basin depend on lithology and, more likely, the composition of the mineral matrix of source rocks in addition to the type and amount of organic matter. Preferential occurrence of normal alkanes when the mineral matrix is clayey [13], formation of i-alkanes in the presence of anhydrous smectite, and the presence of water shifting the composition of generated hydrocarbons toward n-alkane dominated [14] are among the effects of mineral matrix on pyrolysate chemical composition. Espitalie et al. [15] observed the retention of some heavy hydrocarbons by the mineral matrix resulting in underestimation of S_2 and TOC. Dahl et al. [12] quantified the average inert organic carbon plus the two oil- and gas-prone end-members in wt% or TOC unit. Thus, evaluation of the most important parameters in geochemical explorations should be done after taking the mineral matrix effect into account.

2. Geologic setting

In northwest Turkey, the Izmir-Ankara-Erzincan suture and ophiolite zone is considered to be lithospheric remnants of the northern branch of Neotethys. This ocean which separated the Anatolid platform from Eurasia commenced closure along the north dipping subduction zone in the Late Cretaceous, while the initial collision was probably in the Paleocene and continued to the Early Eocene [2].

In the north of the middle Sakarya region, the regression continued from the Late Cretaceous to the Paleocene. The sea became shallower but did not leave the area entirely. In the north of the Göynük basin Late Cretaceous-Eocene marine sediments were continuously deposited, but in the south of the basin fluvial sediments were sandwiched between the Late Cretaceous and Eocene marine sediments [16].

The Upper Cretaceous formations in the Göynük area are the Seben and Tarakli formations. The Senonian Seben Formation is mainly composed of marl, although the occurrence of thin-bedded sandstone intercalation was observed in this study. This unit was deposited under marine conditions and is overlain by the Late Senonian Tarakli Formation, which is composed of fine-grained sandstone deposited in a shallow marine environment. The Tarakli Formation is overlain by the Paleocene Selvipinar Formation, which is mainly composed of reef limestone. Mudstones, marls, oil shales, silt-stones and sandstones of the Paleocene-Eocene Kızılçay Group complete the Tertiary section. The Paleocene-Eocene Kızılçay Group covers a large area in the Göynük Basin. In general red-coloured detrital sediments are charac-teristic of this group. In the current study, the group is divided into three units, namely the Ağsaklar, Kabalar and Dağhacılar formations. The Paleocene Ağsaklar Formation crops out on the north and south wings of the study area. The basal Paleocene Selvipinar Formation is overlain by the fluvial conglomerate, coarse to fine-grained sandstone, siltstone and mud-stone of the Paleocene Ağsaklar Formation. This unit reaches a thickness of 300 m.

The Upper Paleocene Kabalar Formation, which is divided into marl, oil shale and siltstone members and was deposited in a lacustrine environment, conformably overlies the Middle Paleocene Ağsaklar Formation [2]. The marl member is 95 m thick, consisting mainly of green-coloured marl and claystone. This member passes upward into the oil shale member, which is 134 m thick and is composed of shale, marl and sandstone. Siltstone dominated layers are the last member of the Paleocene Kabalar Formation. This member consists of green-coloured siltstone with alternation of the fine-grained sandstone, shale and limestone (Fig. 1).

The Paleocene Kabalar Formation is conformably overlain by the Eocene Dağhacılar Formation, which is composed of red-coloured marl with intercalated sandstone. The Dağhacılar Formation is 300 m thick, and was deposited in a fluvial or delta environment [2].

3. Material and method

A total of 85 oil shale samples of the Kabalar Formation were handpicked from the four stratigraphic sections (HD, KD, DH and DT). During sampling freshly exposed faces were selected.

Samples were crushed, pulverized and then homogenized. Rock-Eval pyrolysis was conducted using the Rock-Eval 6 analyzer manufactured by Vinci Technologies at the Geochemistry Laboratories of the Turkish Petroleum Corporation (TPAO). The analysis yielded several parameters, including S_1, S_2, S_3, TOC and T_{max} (Table 1).
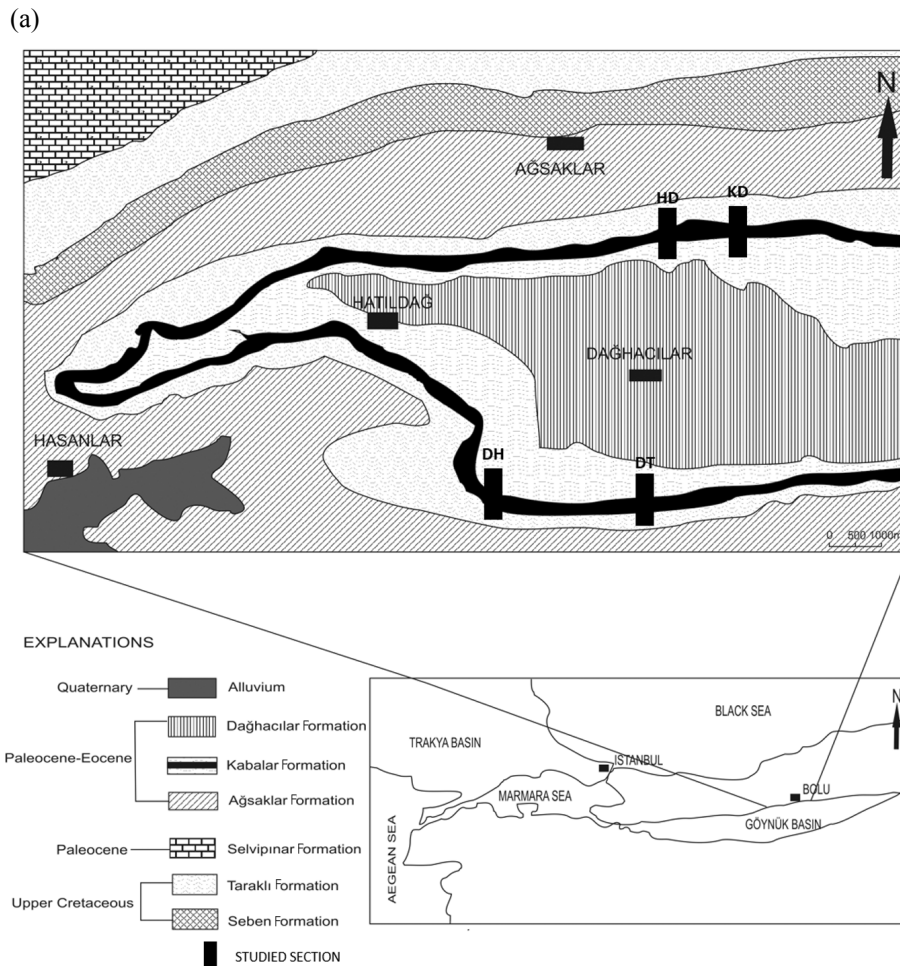
(a)

Fig. 1. The geological map and location of studied sections (a) and generalized stratigraphic section (b) of the studied area. (Modified from [2].)
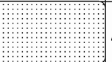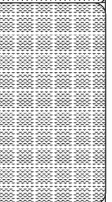
(b)
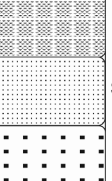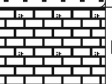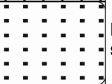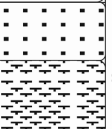
SYSTEM	SERIES	GROUP	FORMATION	MEMBER	THICKNESS, m	LITHOLOGY	EXPLANATION
QUATERNARY					50		Alluvium
TERTIARY	EOCENE	KIZILÇAY	DAĞHACILAR		300		Mudstone
	PALEOCENE		KABALAR	Siltstone	90		Siltstone, shale, mudstone
				Oil shale	134		Black-coloured oil shale
				Marl	95		Marl-mudstone
			AĞSAKLAR		300		Sandstone, siltstone, mudstone
CRETACEOUS	SENONIAN		TARAKLI · SELVİPINAR		100		Reef limestone
					175		Medium- to thick-bedded sandstone
			SEBEN		300		Marl and fine-grained sandstone
							Not to scale

Fig. 1. (Continued).

Table 1. Results of Rock-Eval pyrolysis of studied samples

Sample no	Rock-Eval data	Calculated ratios							
	TOC, wt%	S_1, mg HC/g rock	S_2, mg HC/g rock	S_3, mg CO_2/g rock	T_{max}, °C	HI, mg HC/g TOC	OI, mg CO_2/g TOC	PI	S_2/S_3
DT-7	5.05	0.46	39.56	2.13	439	783	44	0.01	18.6
DT-9	11.68	0.69	91.65	4.07	444	785	35	0.01	22.5
DT-12	4.85	0.18	37.96	2.28	441	783	47	0.01	16.6

Table 1. (Continued)

Sample no	Rock-Eval data	Calculated ratios							
	TOC, wt%	S_1, mg HC/g rock	S_2, mg HC/g rock	S_3, mg CO_2/g rock	T_{max}, °C	HI, mg HC/g TOC	OI, mg CO_2/g TOC	PI	S_2/S_3
DT-15	3.98	0.21	32.56	0.61	442	818	15	0.01	53.4
DT-17	1.28	0.08	5.38	0.7	436	420	55	0.01	7.7
DT-20	8.48	2.04	60.58	4.42	439	714	52	0.03	13.7
DT-23	3.92	0.09	24.64	2.3	437	629	59	0.01	10.7
DT-25	11.37	0.5	91.93	2.7	446	809	24	0.01	34.0
DT-27	6.85	1.17	51.83	2.86	441	757	42	0.02	18.1
DT-28	3.95	0.24	32.73	1.44	440	829	36	0.01	22.7
DT-29	8.78	0.59	52.75	1.86	432	601	21	0.01	28.4
DT-31	9.83	1.85	22.99	7.75	403	234	79	0.07	3.0
DT-32	7.04	0.76	50.93	1.76	439	723	25	0.01	28.9
DT-33	3.22	0.07	21.21	1.52	439	659	47	0.01	14.0
DT-35	5.14	0.52	34.17	2.75	439	665	54	0.01	12.4
DT-38	6.24	2.21	21.16	4.53	406	339	73	0.09	4.7
DT-40	3.3	0.29	25.72	0.47	444	779	14	0.01	54.7
DT-42	7.3	0.87	29.43	2.58	412	403	35	0.03	11.4
DT-44	11.91	0.84	107.25	1.43	448	901	12	0.01	75.0
DT-50	5.19	0.13	40.91	2.52	444	788	49	0.01	16.2
DT-53	1.77	0.04	9.82	0.74	442	555	42	0.01	13.3
DT-54	1	0.04	5.82	0.29	439	582	29	0.01	20.1
DT-56	6.61	0.42	59.93	0.76	446	907	11	0.01	78.9
DT-57	7.72	0.49	63.55	1.82	444	823	24	0.01	34.9
DT-65	7.17	1.04	49.23	3.02	437	687	42	0.02	16.3
DT-70	2.79	0.07	15.33	1.43	438	549	51	0.01	10.7
DT-72	6.71	1.01	37.75	3.8	429	563	57	0.03	9.9
DT-73	8.09	1.3	33.66	5	413	416	62	0.04	6.7
DT-74	1.05	0.07	5.37	0.49	439	511	47	0.01	11.0
DT-76	3.64	0.64	15.9	2.15	412	437	59	0.04	7.4
DT-82	3.97	0.96	17.88	2.05	414	450	52	0.05	8.7
DT-84	5.94	1.32	18.65	3.86	404	314	65	0.07	4.8
DT-90	7.29	1.92	27.1	3.2	412	372	44	0.07	8.5
DT-92	11.15	2.03	92.75	3.13	444	832	28	0.02	29.6
DT-98	3.74	0.53	20.02	1.36	424	535	36	0.03	14.7
DT-99	5.93	2.58	17.39	1.64	397	293	28	0.13	10.6
DH-29	3.49	2.47	24.15	0.57	429	692	16	0.09	42.4
DH-30	5.37	1.98	22.25	2.79	411	414	52	0.08	8.0
DH-33	3.46	1.12	17.42	0.92	410	503	27	0.06	18.9
DH-37	3.21	0.25	18.3	1.15	421	570	36	0.01	15.9
DH-38	2.36	0.55	13.09	0.77	423	555	33	0.04	17.0
DH-41	2.45	1	20.46	0.58	432	835	24	0.05	35.3
DH-42	2.06	0.68	14.19	0.21	433	689	10	0.05	67.6
DH-44	6.46	1.19	57.26	0.75	435	886	12	0.02	76.3
DH-47	2.55	1.16	21.31	0.23	431	836	9	0.05	92.7
DH-50	4.65	0.44	43.24	0.2	441	930	4	0.01	216.2
DH-55	2.89	0.56	18.01	0.3	414	623	10	0.03	60.0
DH-57	4.02	0.43	28.28	0.36	424	703	9	0.01	78.6
DH-59	2.46	0.39	14.2	0.29	416	577	12	0.03	49.0
DH-60	4.46	0.7	42.21	0.37	441	946	8	0.02	114.1
DH-62	3.51	0.82	26.66	0.61	440	760	17	0.03	43.7
DH-64	3.06	1.69	18.36	0.75	415	600	25	0.08	24.5

Table 1. (Continued)

Sample no	Rock-Eval data	Calculated ratios							
	TOC, wt%	S_1, mg HC/g rock	S_2, mg HC/g rock	S_3, mg CO$_2$/g rock	T_{max}, °C	HI, mg HC/g TOC	OI, mg CO$_2$/g TOC	PI	S_2/S_3
DH-66	4.07	2.13	34.93	0.37	438	858	9	0.06	94.4
DH-67	6.47	1.59	54.03	2.1	439	835	32	0.03	25.7
DH-68	1.94	0.28	13.52	0.21	435	697	11	0.02	64.4
DH-70	3.09	0.19	20.62	0.37	439	667	12	0.01	55.7
DH-83	1.54	0.07	9.92	0.43	440	644	28	0.01	23.1
DH-98	8.25	1.27	38.84	5.16	422	471	63	0.03	7.5
DH-101	8.18	0.72	71.94	1.1	442	879	13	0.01	65.4
DH-102	4.38	0.73	18.89	1.94	415	431	44	0.04	9.7
DH-103	2.8	0.89	13.27	0.74	413	474	26	0.06	17.9
DH-105	2.62	0.84	15.9	0.39	426	607	15	0.05	40.8
DH-110	5.17	2.72	35.84	2.05	424	693	40	0.07	17.5
KD-2	13.23	0.86	77.82	4.49	434	588	34	0.01	17.3
KD-25	3.68	0.4	25.82	1.25	442	702	34	0.01	20.7
KD-26	4.11	0.75	34.68	0.55	433	844	13	0.02	63.1
KD-30	3.77	1.43	22.33	0.67	415	592	17	0.06	33.3
KD-31	5.49	1.36	25.45	3.95	416	464	72	0.05	6.4
KD-38	4.75	0.64	26.42	3.17	428	556	67	0.02	8.3
KD-39	3.54	0.56	24.39	0.54	431	689	15	0.02	45.2
KD-42	4.91	0.66	25.17	2.8	422	513	57	0.02	9.0
KD-44	4.55	0.93	18.92	2.8	414	416	62	0.04	6.8
HD-14	9.41	1.18	66.84	2.38	431	710	25	0.02	28.1
HD-17	4.46	1.12	36.86	0.72	437	826	16	0.03	51.2
HD-21	2.56	0.12	13.77	1.56	433	538	61	0.01	8.8
HD-22	1.64	0.28	9.58	0.57	438	584	35	0.03	16.8
HD-23	4.19	0.2	29.43	1.94	437	702	46	0.01	15.2
HD-25	3.54	1.06	24.34	0.35	428	688	10	0.04	69.5
HD-27	4.4	0.32	33.1	0.5	438	752	11	0.01	66.2
HD-29	6.81	0.68	25.3	5.69	410	372	84	0.03	4.4
HD-32	3.57	0.17	24.06	0.81	441	674	23	0.01	29.7
HD-38	3.95	0.3	22.92	1.28	434	580	32	0.01	17.9
HD-45	6.38	0.95	31.98	3.87	426	501	61	0.03	8.3
HD-47	6.39	0.61	54.6	1.27	441	854	20	0.01	43.0
HD-50	7.51	2.56	62.3	1.57	443	830	21	0.04	39.7

A flame ionization detector (FID) was used to measure the concentration of organic compounds generated during pyrolysis. The first peak S_1 represents hydrocarbons that can be thermally distilled from a rock. The second peak S_2 represents hydrocarbons generated by the pyrolytic degradation of the kerogen in the rock. The third peak S_3 stands for the carbon dioxide generated during temperature programming up to 390 °C, and is analyzed using a thermal conductivity detector (TCD). The hydrogen index (HI) corresponds to the quantity of pyrolyzable organic compounds from S_2 relative to the TOC in the samples (mg HC/g TOC) and can be successfully used to assess the oil generation potential of the rock and the type of organic matter.

The oxygen index (OI) is indirectly related to the quantity of terrestrial organic matter in the sample (S_3/TOC).

More details of this method can be found in [17–19].

4. Discussion

4.1. Source rock characteristics

The amount of organic matter (OM) in rocks is usually measured as total organic carbon content (TOC) and expressed as a weight percentage of a dry rock [20]. Samples from the Kabalar Formation exhibit high TOC values ranging from 1 to 13.23 wt%, with an average of about 5.07 wt% (Table 1). These values indicate a source rock with a good to excellent source rock potential [19]. However, sediments with high organic carbon contents are not necessarily a potential source for oil. Waples [21] suggests that black organic shales with a TOC less than about 2 wt% may be deposited in waters with some oxygen.

The kerogen type can be evaluated by using a cross plot of hydrogen index vs oxygen index and S_2/S_3 ratio [19, 22]. Peters and Cassa [19] classified samples with an S_2/S_3 ratio greater than 10 as oil prone kerogen (types I and II) bearing samples. They also suggested that samples with an S_2/S_3 ratio lower than 5 contain gas prone organic matter (type III kerogen). Generally results from Rock-Eval pyrolysis revealed that the overwhelming majority of Kabalar oil shale samples are composed of type I and II kerogen. On the plot of HI vs T_{max} and OI, almost all of the samples are located in the field of kerogen type I and II (Figs. 2 and 3) whereas using the S_2/S_3 ratio of Kabalar oil shale samples, it might be inferred that type III organic matter is also a contributor to TOC (Table 1).
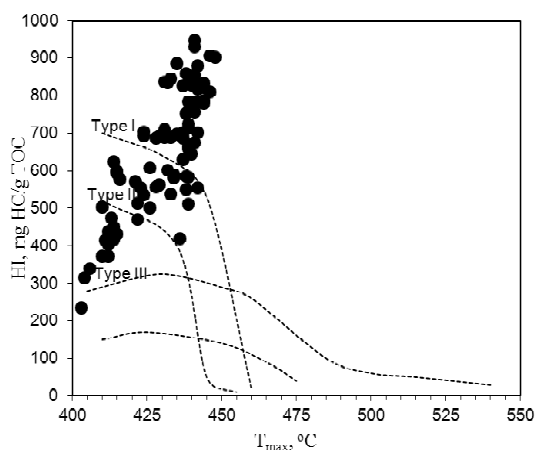

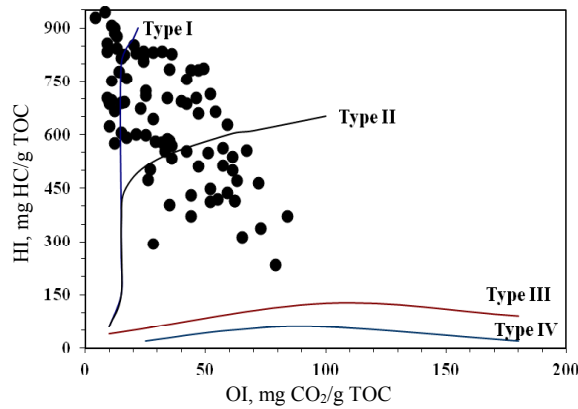Fig. 2. HI vs T_{max} plot for the Kabalar Formation.

Fig. 3. Rock-Eval HI vs OI plot indicating that Kabalar oil shale samples are dominated by oil prone organic matter (type I and II kerogen).

Microscopic studies for selected oil shale samples (Table 2) define an organic matter assemblage consisting predominantly of alginite and amorphous material [23] which shows apparently a higher proportion of type I kerogen relative to the inferred proportion from Rock-Eval data and especially S_2/S_3 ratios. The discrepancy is believed to have been caused by the mineral matrix retention effect discussed below in part 4.2.

The HI vs TOC diagram shows all but one of the samples to have a good to excellent oil source potential (Fig. 4).

The level of thermal maturation can be evaluated using various parameters, including T_{max} (i.e. the temperature at which the maximum amount of S_2 hydrocarbons are generated during the assay), spore color index (SCI) and S_2/S_3 ratio. Low T_{max} values (< 440 °C) indicate immature organic
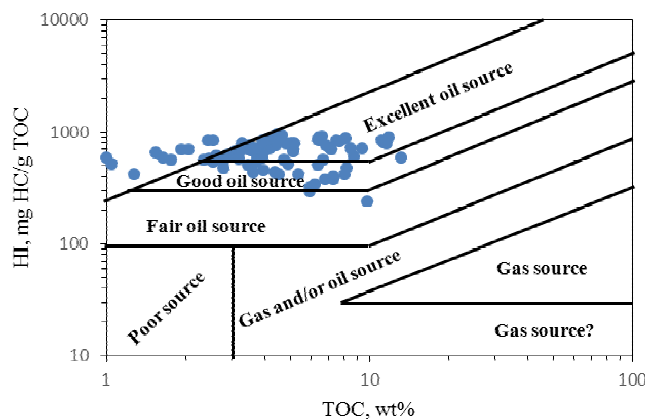

Fig. 4. HI vs TOC diagram for the studied Kabalar Formation indicating a good to excellent source rock potential.

material whereas high values (> 448 °C) imply the condensate and wet gas zone for samples containing predominantly type I kerogen [24]. The T_{max} value of Kabalar oil shale is between 397 and 448 °C. Plotting the results on the PI vs T_{max} diagram suggests the majority of samples are immature (Fig. 5).
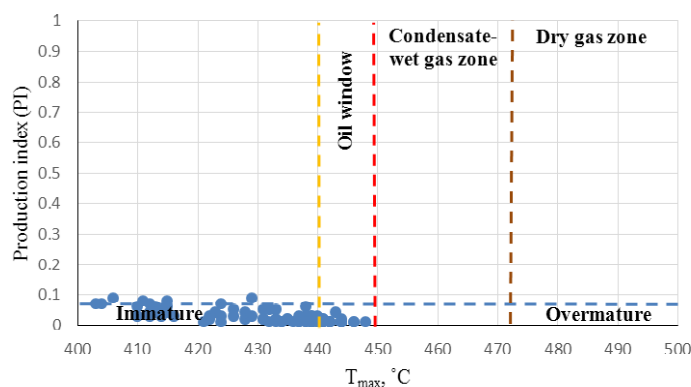

Fig. 5. T_{max} vs PI plot for the studied Kabalar oil shale samples showing them to be in the immature to early mature stages of thermal maturity.

Although some samples are in the oil window, based on the plot of S_1 vs TOC (Fig. 6) and low PI values (Table 1), it seems that no amount of generated Kabalar oil is migrated out [25].

Scanning electron microscopic (SEM) studies of shale samples by Sarı and Aliyev [11] also show the presence of morphological structures interpreted to be of hydrocarbon droplets.

The spore color index (SCI) of oil shale samples ranges from 2.5 to 3 (Table 2) indicating that the samples are immature to early mature and have not reached peak oil generation [26], which is also supported by low values of production index (PI).

Peters [27] applied S_2/S_3 ratio as a maturity indicator and classified samples with an S_2/S_3 ratio greater than 8 as immature or early mature and suggested that lower values (< 8) imply higher levels of maturity. The S_2/S_3 values of Kabalar oil shale samples are generally greater than 8, indicating that the samples are immature to early mature.

In a previous study by Sarı and Aliyev [11], due to limited sampling, the source potential and the level of maturity of the Kabalar Formation have been under- and overestimated, respectively. They classified this unit as having a fair oil source potential which is in the early to middle stages of thermal maturity.
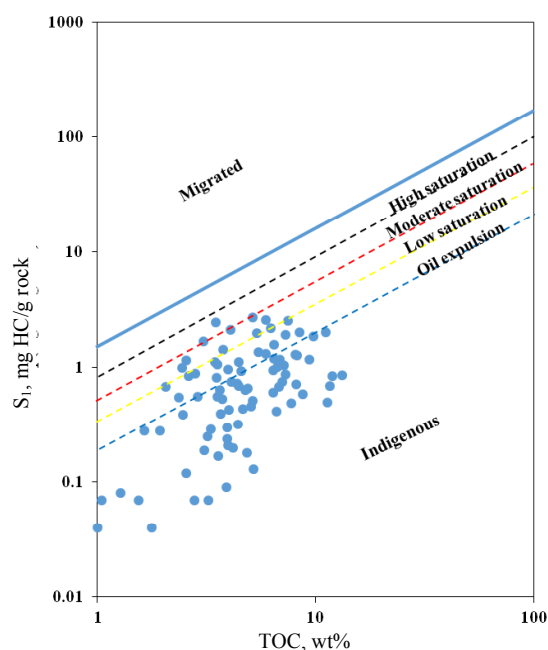
Fig. 6. Plot of S_1 vs TOC. The field above the solid line refers to migrated hydrocarbons, below, to indigenous hydrocarbons. The plot suggests that no migration of hydrocarbons into oil shale has taken place. (Ranges are from [25].)

Table 2. Organic petrographic results for the Kabalar Formation [23]

Sample	Amorphous + algae, %	Exinite, %	Vitrinite, %	Oxidized materials, %	SCI*
DH-30	15	80	–	5	2.5–3
DH-33	95	5	–	–	3
DH-37	95	5	–	–	3
DH-44	95	5	–	–	2.5–3
DH-47	100	–	–	–	3
DH-55	95	5	–	–	3
DH-60	100	–	–	–	3
DH-62	100	–	–	–	3
DH-64	100	–	–	–	3
DH-67	90	10	–	–	-
DH-98	100	–	–	–	3
DH-102	95	5	–	–	3
DH-103	100	–	–	–	3
DH-105	100	–	–	–	3
DH-110	100	–	–	–	3
HD-14	100	–	–	–	3
HD-17	100	–	–	–	3
HD-21	100	–	–	–	3
HD-23	–	–	–	–	2.5
HD-25	100	–	–	–	2.5–3
HD-27	100	–	–	–	3
HD-29	100	–	–	–	3
HD-32	85	15	–	–	3
HD-45	100	–	–	–	3
HD-50	100	–	–	–	–

* SCI – Spore Color Index

4.2. Matrix effect correction

An S_2 vs TOC chart is a valuable means to interpret Rock-Eval pyrolysis data and quantitatively estimate the matrix effect and inert carbon [12]. The retention of hydrocarbons by the mineral matrix could be a source of under-estimation. Although the mineralogy and structure of clay minerals have a key role in estimating mineral matrix effect, Espitalie et al. [15] have pointed out that this effect reaches its maximum for samples which show a lower level of maturity. Retention is more intense when the matrix is clayey (especially illite). As the amount of organic carbon (TOC), T_{max} and proportion of carbonates in the mineral matrix network increase, the retention is minimized [28]. In order to evaluate the effect of mineral matrix, select the appropriate GORP overlay and take the possibility of kerogen transformation into account, the samples were divided into mature and immature subdivisions. With regard to the algal (type I) nature of kerogen in the studied samples, the samples with $T_{max} \geq 440$ °C were considered mature [24]. The results were separately plotted on the S_2 vs TOC diagram (Fig. 7). In an ideal case, the line intersects through the origin but resulting from the mineral matrix retention effect and inert carbon [15, 22], the trend line offsets from the origin and intersects through the positive side of the TOC-axis.

4.2.1. Immature subdivision

To obtain the proportion of inert carbon, at first the amount of retained hydrocarbons should be calculated. The equation of the regression line (S_2 vs TOC plot) is basically as follows (Eq. 1):

$$Y = aS_2 + b \tag{1}$$

For immature samples the obtained equation is as follows:

$$Y = 0.1287x + 1.238 \tag{2}$$

Using the slope ($a = 0.1287$) and TOC intersection point ($b = 1.238$), it is possible to calculate $TOC_{(inert)}$ and $HI_{(live)}$ (Eqs. 3, 4, 5):

$$HI = \frac{100}{a} \quad \text{or} \quad 100S_2/TOC_{(live)} \tag{3}$$

$$TOC_{(inert)} = TOC_{(\text{intersection point in Y axis or } b \text{ in Eq. 1})} - TOC_{(retained)} \tag{4}$$

$$TOC_{(live)} = (TOC_{(\text{observed or mean})} + TOC_{(retained)}) - TOC_{(inert)} \tag{5}$$

Dahl et al. [12] suggested that the negative intersection with the S_2 axis indicates the average magnitude of hydrocarbons retained by the mineral matrix. To quantify the amount of retention, the intersection point where the regression line passes from the S_2 axis (X axis) is multiplied by the stoichiometric factor (α). Using elemental analysis, Tissot and Welte [17]

calculated the mean value of this factor 0.084. In the immature subdivision of the Kabalar Formation, there is an intense retention (mineral matrix effect). After correcting the mineral matrix effect the mean HI value increased by about 268 mg HC/g TOC (Table 3).
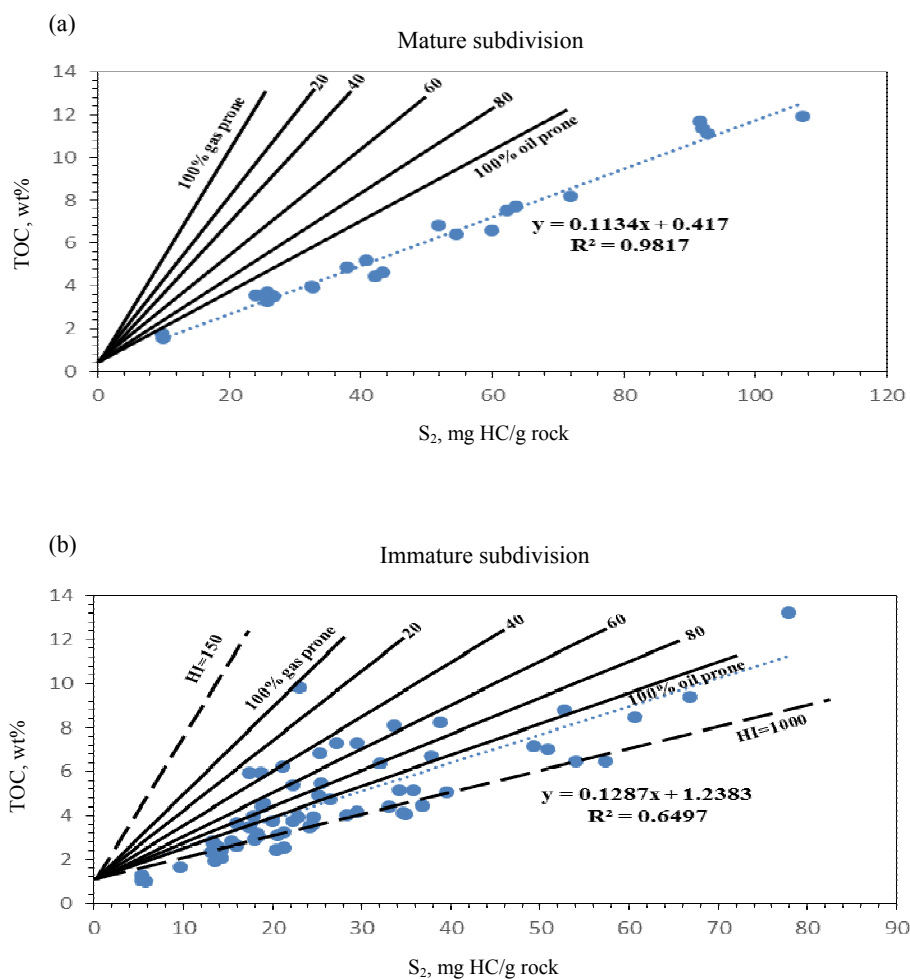
(a)

Mature subdivision

$y = 0.1134x + 0.417$
$R^2 = 0.9817$

(b)

Immature subdivision

$y = 0.1287x + 1.2383$
$R^2 = 0.6497$

Fig. 7. Plots of S_2 vs TOC for mature (a) and immature (b) subdivisions. The overlay is superimposed on the plot to read the kerogen mixture (GORP). The intensity of retention is minimized in the mature subdivision, indicating minimization of the matrix effect in samples of higher thermal maturity.

Table 3. Pyrolysis values before (HI$_{mean}$) and after matrix effect correction (HI$_{live}$)

Formation	Sub-division	HI$_{(mean)}$	HI$_{(live)}$	S$_{2(mean)}$	S$_{2(adsorb)}$	TOC$_{(mean)}$ [*]	TOC$_{(adsorb)}$	TOC$_{(inert)}$ [**]	TOC$_{(live)}$ [***]
Kabalar	Immature	587	855	27.13	9.67	4.72	0.812	0.42	4.3
Kabalar	Mature	799	898	49.97	3.69	6.08	0,309	0.1	5.98

[*] TOC$_{(mean)}$ = TOC$_{(live)}$ + TOC$_{(inert)}$ (primary).

[**] TOC$_{(inert)}$ − after deducting retained hydrocarbons. Based on trend line equations in Fig. 5 (the intersection point with TOC axis) primary values are 1.23 and 0.41 for immature and mature samples, respectively.

[***] TOC$_{(live)}$ was calculated using the values of 0.425 and 0.107 as inert carbon proportion in immature and mature samples, respectively.

4.2.2. Mature subdivision

In case of mature subdivision the mineral matrix retention effect is highly reduced (Eq. 6). The difference can be a strong indicator of the thermal maturity effect on the retention of hydrocarbons by the mineral matrix:

$$Y = 0.1134x + 0.417 \qquad (6)$$

In addition to maturity, the amount of retention may also be influenced by the mineralogy of the matrix. The mineral matrix in Kabalar oil shale samples is mainly composed of a mixture of clay and carbonate minerals [23], which increases the retention of hydrocarbons.

4.3. Kerogen quality assessment using GORP factor

The GORP factor enables the geochemist to fill in the gaps and assess the average oil and gas producing constituents in source rocks when pyrolysis GC and visual kerogen data are scarce. In order to divide the live TOC and S$_2$ into oil prone and gas prone members, at first the TOC$_{(live)}$ value of the mature subdivision was restored back to its original value (before transformation of kerogen) (Eq. 9). Using Equation 7, the transformation ratio (TR) for the mature subdivision is 0.2. S$_{2(restored;\ lost)}$ and TOC$_{(restored)}$ were calculated employing Equations 8, 9 and 10:

$$TR = (HI_{(original\ /\ immature\ sample)} - HI_{(present)}) / HI_{(original\ /\ immature\ sample)} \qquad (7)$$

$$S_{2(lost)} = S_{2(observed)} \times [TR / (1\text{-}TR)] \qquad (8)$$

$$S_{2(restored)} = S_{2(observed)} + S_{2(lost)} \qquad (9)$$

$$TOC_{(restored)} = TOC_{(observed)} + \{S_{2(lost)} \times \alpha\} \qquad (10)$$

With regard to TR, the appropriate S$_2$ vs TOC overlay for each subdivision was selected. For both subdivisions the factor obtained is 0 (Fig. 7). Thus, it

can be inferred that $TOC_{(live)}$ of Kabalar oil shale is composed only of oil prone material. This conclusion is in agreement with organic petrographic observations (Table 3). Also the chaotic pattern of the S_2 vs TOC plot in the immature subdivision is related to fluctuations in environment conditions. According to Sarı and Koç [23] the depositional environment of Kabalar oil shale is a shallow marine environment with seasonal fluctuation in sea level.

Now it is possible to calculate the proportion of TOC (oil/II) and TOC (gas/III), according to Equations 11 and 12:

$$TOC\ II = TOC \times (1\text{-}GORP) \qquad (11)$$

$$TOC\ III = TOC \times GORP \qquad (12)$$

Final results are presented in Table 4. The values in parentheses are the values obtained before correcting the matrix effect. Comparing the values, the role of the matrix effect in leading to underestimation of the hydrocarbon potential becomes obvious.

Table 4. Gross kerogen components in TOC units separately for each subdivision. (Oil and gas potentials and intermediate results assessed from the GORP factor calculation in the Göynük area. The values in parentheses are values obtained before correcting the matrix effect.)

Parameter	Immature subdivision	Mature subdivision
$TOC_{(observed)}$	4.72	6.08
$S_{2(observed)}$	27.13	49.97
TR	0	0.2
$S_{2(restored)}$	–	62.46
GORP	0	0
$TOC_{(restored)}$	4.72	7.12
TOC II	4.3 (3.49)	7.02 (6.71)
TOC III	0	0 (0)
TOC IV	0.42 (1.23)	0.1 (0.41)
$S_{2(oil)}$	36.8 (27.13)	66.15 (62.46)
$S_{2(gas)}$	0 (0)	0 (0)

5. Conclusions

Pyrolysis results suggest that the kerogen of oil shale in the Kabalar Formation is mainly of type I and type II, which is supported by organic petrographic studies. The average TOC content of the Kabalar Formation is 5.07 wt%, which implies a good to excellent source rock potential. With an average of about 644 mg HC/g TOC, HI values suggest a good to excellent oil source potential. Based on T_{max}, PI, SCI values and S_2/S_3 ratios, oil shale samples of the Kabalar Formation are in the immature to early mature stages of thermal maturity.

There is an intense mineral matrix retention effect especially in the immature subdivision of the Kabalar Formation. After correcting the matrix

effect in this subdivision the mean HI value (ca 587 mg HC/g TOC) increased by about 268 mg HC/g TOC. Comparison of S_2 vs TOC graphs of subdivisions gives evidence of the apparent role of maturity in the adsorption of hydrocarbons by the mineral matrix. The amount of retained S_2 sharply decreased in the mature subdivision and the correlation coefficient of the regression line increased by more than 30%. Using an appropriate overlay, the GORP factor was obtained 0 (100% oil prone) for both subdivisions, which is in agreement with results from Rock-Eval pyrolysis and microscopic studies.

REFERENCES

1. Ediger, V. S., Tatlıdil, H. Forecasting the primary energy demand in Turkey and analysis of cyclic patterns. *Energ. Convers. Manage.*, 2002, **43**(4), 473–487.
2. Şener, M., Şengüler, İ. Geological, mineralogical and geochemical characteristics of oil shale bearing deposits in the Hatıldağ oil shale field, Göynük, Turkey. *Fuel*, 1998, **77**(8), 871–880.
3. MTA, General Directorate of Mineral Research and Exploration. *Lignite, Asphaltite, Hard Coal, Oil Shale and Uranium Reserves in the World and in Turkey*. MTA Report, 1993. MTA, Ankara, Turkey (in Turkish).
4. Kök, M. V., Sengüler, I., Hufnagel, H., Sonel, N. Thermal and geochemical investigation of Seyitömer oil shale. *Thermochim. Acta*, 2001, **371**(1–2), 111–119.
5. Şener, M., Şengüler, I., Kök, M. V. Geological considerations for the economic evaluation of oil shale deposits in Turkey. *Fuel*, 1995, **74**(7), 999–1003.
6. Tekin, E., Sarı, A. Morphology of hydrocarbon droplets from bituminious shales of the Kabalar Formation (Göynük-Bolu). *Geosound*, 1999, **35**, 1–13 (in Turkish).
7. Akkus, I., Sümer, A., Sengüler, I., Taka, M., Pekatan, R. *The Drill Logs of Beypazari-Çayirhan Oil Shale Field*. MTA Report, 1982. MTA, Ankara, Turkey (in Turkish).
8. Saner, S. The depositional associations of Upper Cretaceous-Paleocene-Eocene Times in Central Sakarya and petroleum exploration possibilities. In: *Proceed. Fourth Petroleum Congress of Turkey*, 1978, 83–95 (in Turkish).
9. Hufnagel, H. *Investigation of Oil Shale Deposits in Western Turkey*. Technical Report, Part 2. Project No. 84.2127.3. BRG, Hannover, 1991.
10. Çimen, O., Koç., Ş., Sarı, A. Rare earth element (REE) geochemistry and genesis of oil shales around Dağhacılar village, Göynük-Bolu, Turkey. *Oil Shale*, 2013, **30**(3), 419–440.
11. Sarı, A., Aliyev, S. A., 2005. Source rock evaluation of the lacustrine oil shale bearing deposits, Göynük/Bolu,Turkey. *Energ. Source.*, 2005, **27**(3), 279–298.
12. Dahl, B., Bojesen-Koefoed, J., Holm, A., Justwan, H., Rasmussen, E., Thomsen, E., 2004. A new approach to interpreting Rock-Eval S_2 and TOC data for kerogen quality assessment. *Org. Geochem.*, 2004, **35**(11–12), 1461–1477.
13. Jurg, J. W., Eisma, E. Petroleum hydrocarbons: generation from fatty acid. *Science*, 1964, **144**(3625), 1451–1452.

14. Almon, W. R. *Petroleum-Forming Reactions: Clay Catalyzed Fatty Acid Decarboxylation*. PhD Thesis, Univ. Missouri-Columbia, 1974, 135 pp.
15. Espitalie, J., Madec, M., Tissot, B. Role of mineral matrix in kerogen pyrolysis: influence on petroleum generation and migration. *Am. Assoc. Petr. Geol. B.*, 1980, **64**(1), 59–66.
16. Saner, S. Paleogeography interpretation and qualification of Mudurnu-Göynük Basin after the deposition of the Jurassic. *Bull. Geol. Soc. Turkey*, 1980, **23**, 39–52 (in Turkish).
17. Tissot, B. P., Welte, D. H. *Petroleum Formation and Occurrence: A New Approach to Oil and Gas Exploration*. Springer, Berlin, 1978, 583 pp.
18. Lafargue, E., Marquis, F., Pillot, D. Rock-Eval 6 applications in hydrocarbon exploration, production, and soil contamination studies. *Rev. I. Fr. Petrol.*, 1998, **53**(4), 421–437.
19. Peters, K. E., Cassa, M. R. Applied source rock geochemistry. In: *The Petroleum System – From Source to Trap* (Magoon, L. B., Dow, W. G., eds.), American Association of Petroleum Geologists Memoir 60, Tulsa, OK, 1994, 93–119.
20. Maravelis, A., Zelilidis, A. Organic geochemical characteristics of the late Eocene–early Oligocene submarine fans and shelf deposits on Lemnos Island, NE Greece. *J. Petr. Sci. Eng.*, 2010, **71**, 160–168.
21. Waples, D. W. Reappraisal of anoxia and organic richness, with emphasis on Cretaceous of North Atlantic. *Am. Assoc. Petr. Geol. B.*, 1983, **67**(6), 963–978.
22. Langford, F. F., Blanc-Valleron, M. M. Interpreting Rock-Eval pyrolysis data using graphs of pyrolizable hydrocarbons vs. total organic carbon. *Am. Assoc. Petr. Geol. B.*, 1990, **74**(6), 799–804.
23. Sarı, A., Koç, S. *Scientific Investigation and Economic Potential of Bituminous Shale Field in Bolu-Göynük-Hasanlar and Suburbs (Hatıldağı), Turkish Coal Institute*. Internal report, No.1, 2012 (in Turkish).
24. Espitalie, J., Deroo, G., Marquis, F. (1985). La pyrolyse Rock-Eval et ses applications. *Rev. I. Fr. Pétrol.*, Part I, 1985, **40**(5), 563–578, Part II, **40**(6), 755–784, Part III, 1986, **41**(1), 73–89.
25. Jin, H., Sonnenberg, S. A. Source Rock Potential of the Bakken Shales in the Williston Basin, North Dakota and Montana. *Poster session presented at American Association of Petroleum Geologists Annual Convention and Exhibition*, Long Beach, California, USA, April 22–25, 2012.
26. Collins, A. The 1–10 Spore Colour Index (SCI) scale: a universally applicable colour maturation scale, based on graded, picked palynomorphs. *Mededelingen Rijks Geologische Dienst*, 1991, **45**, 39–47.
27. Peters, K. E. Guidelines for evaluating petroleum source rock using programmed pyrolysis. *Am. Assoc. Petr. Geol. B.*, 1986, **70**(3), 318–329.
28. Hunt, J. M. *Petroleum Geochemistry and Geology*, 2nd ed. W. H. Freeman and Company, New York, 1996.